Journal of Computer-Aided Molecular Design (2005) 19: 259–269
DOI 10.1007/s10822-005-4994-5

An effective simulation of aqueous micellar aggregates by computational models

Guido Angelini[a], Giorgio Cerichelli[b], Simona Cerritelli[c], Marco Pierini[d,*], Gabriella Siani[a] & Claudio Villani[d]

[a]*Dipartimento di Scienze del Farmaco, Università "G. d'Annunzio", Via dei Vestini 31, 66013, Chieti, Italy;* [b]*Dipartimento di Chimica, Ingegneria Chimica e Materiali, Università degli Studi dell'Aquila,Via Vetoio, Coppito Due (AQ), Italy;* [c]*Institute for Biological Engineering & Biotechnology, Swiss Federal Institute of Technology (EPFL) Lausanne, LMRP, CH-1015, Lausanne, Switzerland;* [d]*Dipartimento di Studi di Chimica e Tecnologia delle Sostanze, Biologicamente Attive Università degli Studi "La Sapienza", P.le A. Moro 5, Roma, ltaly*

Received 8 October 2004; accepted 4 April 2005

Key words: complexation induced shift, ^{1}H-NMR shift prediction, micellar aggregates models, molecular docking, molecular recognition

Summary

We have computationally studied the interaction modes, localization and orientation of a benzene (Bz) molecule on the surface of micelles formed by cetyltrimethylammonium salts CTAX. Experimental ^{1}H-NMR data on complexation shifts induced by Bz on the polar head hydrogens and on the adjacent methylene hydrogens of CTAX have been interpreted using a computational approach that combines an automatic molecular docking procedure with a calculation module that accounts for NMR complexation shifts due to ring current diamagnetic anisotropy. Three different models were used to reduce the complexity of the micellar system. Computational results, in good agreement with available experimental data, point to a preferential localization of the Bz molecule along the CTAX alkyl tail, about 3.9 Å away from the charged nitrogen. The Bz molecular plane is predicted perpendicular to the C—H bonds of the alkyl tail. The good results obtained with the simplest model suggest that it could be used to study more complex systems involving surfactants endowed with molecular recognition or catalytic abilities.

Introduction

Computational methods can have an important role in the elucidation of structural and reactivity features of molecular entities. Several approaches, like molecular modeling and QSAR techniques, can be either used as an aid in interpreting experimental data (e.g. NMR, UV, CD, IR spectroscopy data) or as predictive tools for kinetic, geometric and thermodynamic properties. Recent applications of molecular modeling are focused on supramolecular systems and on molecular docking algorithms [1, 2]. Within this framework, the main efforts are aimed at the rational development of drug substances (inhibitors or agonists) having biomacromolecules as targets [3–6], and at a deeper understanding of the molecular recognition mechanisms with particular interest in those systems where chirality is actively involved (chiral recognition) [2, 7].

An interesting field of supramolecular chemistry where computational approaches are expected to give interesting results is that related to micellar or vesicular aggregates spontaneously formed in water by surfactants. The ability of these systems

*To whom correspondence should be addressed. Fax: +39-06-4991-2780,; E-mail: marco.pierini@uniroma1.itf

to greatly enhance the water solubility of hydrophobic molecules has been the subject of several studies that have led to their use in a number of applications [8–12].

Within this context it is of paramount importance to have a detailed picture of the interaction modes of the solute molecules with the surface of the aggregates, including geometric and energetic description of the supramolecular system [13–15]. The structural and dynamic complexities of micellar and vesicular systems generated in aqueous media require an integrated approach where experimental results are confronted with theoretical data generated by simple models of the real system.

Here we report a computational study on systems composed by an aqueous aggregate of cetyltrimethylammonium salts, CTAX, and a benzene (Bz) molecule. These systems were examined experimentally by looking at the ^{1}H-NMR chemical shift variations observed for some of the alkyl hydrogens of CTAX in the presence of Bz. The computational counterpart of the work consists in (i) the generation of model systems in which the CTAX components are held fixed in space while one Bz molecule explores their surfaces guided by an exhaustive, automatic docking procedure; and (ii) the calculation of the ^{1}H-NMR shielding of the polar head hydrogens and of the adjoining methylene hydrogens of CTAX due to the diamagnetic anisotropy of the Bz ring.

Experimental procedure for the calculation of induced chemical shift

Several examples exist of organic molecules having hydrogens positioned over an aromatic ring. ^{1}H-NMR chemical shift, δ_H, of these hydrogens is moved upfield, as a result of their position relative to the shielding cone of the ring where they experience the diamagnetic effects of the π-electrons ring current [16–20]. In the classic framework, a quantitative estimate of these effects can be obtained by a number of approaches, including the simple equivalent dipole model and the more sophisticated double-loop and double-dipole models [20–24]. When considering the formation of supramolecular systems, diamagnetic anisotropy effects due to aromatic rings are of particular interest, as they can yield information on the relative disposition of the assembling molecular units in the complexes [25, 26]. Such a situation is well illustrated by the results of a recent multinuclear NMR investigation on the solubilization of Bz in aqueous solutions of cetyltrimethylammonium surfactants: ^{1}H chemical shifts of the headgroup signals and of four methylenes of the aliphatic chain were seen to undergo larger upfield shifts upon Bz addition, compared to the hydrophobic tail signals [27]. More specifically, variation of the δ_H data for the water solubilization of Bz by cetyltrimethylammonium salts, CTAX, (X = Br^-, Cl^-, NO_3^-, $CH_3SO_3^-$ and $(SO_4)^{2-}{}_{1/2}$ abbreviated hereinafter CTAB, CTAC, CTAN, CTAMs and CTAS respectively) were reported and are used in the present work. The upfield shifts of the methyl headgroup hydrogens H1′, as well as those of the four adjacent methylenes in the cetyl chain H1, H2, H3 + 4 (see Figure 1) are diagnostic of the mode of interaction of the Bz probe with the micellar surface.

We used these data to determine the position and the average orientation of the Bz ring in the micelle, following a computational three-step approach:

Step1 – modeling the micellar aggregate without counterions

Step2 – search of the most significative minimum energy geometries for the supramolecular systems formed by one Bz molecule and the micelle models

Step3 – calculation of the ^{1}H-NMR upfield shifts for H1′ and H1–4 using the equivalent dipole model, and comparison with experimental values.

Computational methods

1. (a) Conformational search of CTA was carried out by Batchmin and Macromodel version 4.5 (Columbia University, NY) using the following options: MM2* Force Field, Montecarlo stochastic algorithm with 3000 generated structures, minimization by PR conjugate gradient. All the rotatable bonds were explored. Structures generated were further optimized with the MMX force field (PC Model 4.0, Serena Software, Bloomington, IN) and the lowest energy conformation was employed as selector in the next docking step performed with the program MolInE [28]; (b) MMX force field and a dielectric constant ϵ = 80 (PC Model

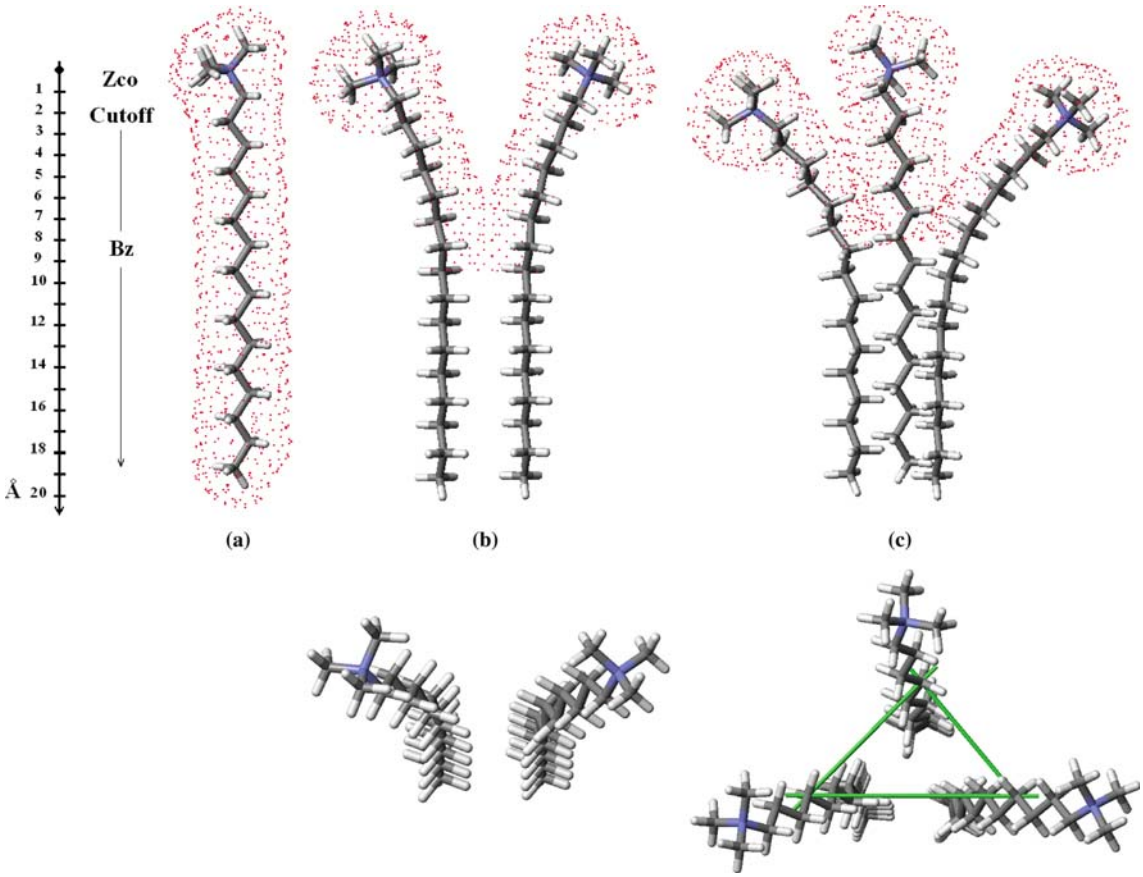

Figure 1. Pictures of the micellar aggregate molecular models used in this work. Dots on the van der Waals surfaces represent regions where the contact in between Bz and micellar models were considered in the docking procedure. (a) Mod-*1*-CTA; (b) Mod-*2*-CTA; (c) Mod-*3*-CTA.

4.0, Serena Software, Bloomington, IN); (c) dielectric constant $\epsilon = 80$ and MMX force field as implemented in MolInE docking program [28].

2. The stand-alone computer program is available on request by e-mail at the address marco.pierini@uniroma1.it.
3. Calculations were performed by ACD/HNMR Predictor v.4.56, 90 Adelaide Street West Toronto, Ontario M5H 3V9, Canada.
4. CAT is a computer program planned to aid conformational analysis studies. The recognition of duplicated structures is achieved in two steps:

(i) the geometries to be compared are automatically aligned by rotating their overall structure in such a way that the principal moments of inertia, calculated on a selected substructure, are brought in a univocal coincidence;

(ii) the root-mean-square deviation (RMS) between a subset of atoms is computed; the compared geometries are considered as twins if the RMS value is less than an imposed cutoff value.

In this work the principal moments of inertia were calculated on the geometrically invariant micellar model portion of every adduct and the RMS was evaluated between all the atoms of the aggregates.

Models used to simulate the micellar aggregate

The large number of surfactant units involved in the formation of each micellar aggregate requires an highly approximate model that is easy to handle computationally and that gives, at the same time, reliable results in terms of predicting power for the ^{1}H-NMR shifts considered in our systems.

Thus, we choose to examine three limiting models consisting of 1, 2 or 3 units of the cetyltrimethylammonium cation, CTA.

Model Mod-1-CTA

The structure of CTA, selected as a minimum energy conformation obtained by conformational search and optimization using a molecular mechanics method (see subsection 1a in Computational Methods), is employed as a target for the docking simulations with the Bz molecule. Each supramolecular adduct Mod-*1*-CTA//Bz generated in the molecular docking (Step2) is placed in a Cartesian reference system, with its cationic head nitrogen on the origin and the alkyl tail oriented along the z axis and pointing away from the charged head (Figure 1a). The maximum movement allowed to the Bz probe along the alkyl chain and the chemical shift calculation are controlled and performed by an algorithm developed inhouse and translated in a computer executable package (see subsection 2 in Computational Methods). To this purpose a cut-off value Z_{CO} is chosen so that only those supramolecular adducts where the distance between the origin and the centre of mass of Bz is less than Z_{CO} are considered. The $\Delta\delta_H$ values (difference between the δ_H with and without Bz, Step 3), are computed for H1′ and H1–4 as a mean weighted on the Boltzmann populations of the selected adducts.

Model Mod-2-CTA

Two structural subunits of CTA, obtained in the same way as described for Mod-*1*-CTA, are placed with the alkyl tails in close contact and with their polar heads side by side. The overall geometry of the dimeric aggregate is optimized by molecular mechanics (see subsection 1b in Computational Methods). The dimer Mod-*2*-CTA, characterized by a C2 symmetric structure (Figure 1b), is then used in the second step as a substrate for the docking with the Bz molecule. During the third step, $\Delta\delta_H$ values are calculated only for those supramolecular adducts containing: (a) the Bz molecule located in the region of space between the two alkyl tails of CTA; (b) the Bz molecule located over the surface of the headgroup methyls of CTA (Figure 1b). This selection eliminates the contribution of Bz molecules that, in the real micellar system, are not free to slide over the entire length of the alkyl tails as a result of geometrical and steric constraints. The CTA dimeric model simulates the generation of temporary cavities, accessible to Bz, in the dynamically evolving micellar surface by a static 'push away' effect between the polar heads. This assumption is consistent with the results of molecular dynamics simulations of micellar aggregates in water [29, 30]. In these studies, the calculated contribution to the micellar accessible surface area from both the headgroups (Sa_{heads}) and the tails (Sa_{tails}) points to a sizeable role played by the hydrocarbon portion (Sa_{heads}/Sa_{tails} ratio is ranging from 24 to 41), and this turn out true either before and after the micelle equilibration. In Mod-*2*-CTA, the estimated Sa_{heads}/Sa_{tails} ratio (25) agrees well with the reported values, suggesting the model can be considered as a snapshot of a little, elementary micellar surface portion.

Model Mod-3-CTA

This model is built as for the dimeric model, using three CTA subunits with their alkyl tails aligned and in close contact, and with the polar heads placed side by side. The obtained structure has only apparent 3-fold symmetry, as shown by a cross section of the aligned tails (Figure 1c). Also in this case $\Delta\delta_H$ values were calculated only for those supramolecular adducts having the Bz molecule over the polar heads or between the alkyl tails (Figure 1c) to simulate the Bz diffusion among the floating cavities. The estimated Sa_{heads}/Sa_{tails} ratio for Mod-*3*-CTA is 30.

Generation of the supramolecular adducts Mod-*n*-CTA//Bz

The formation of two- three- and four-bodies adducts containing the Bz molecule as selectand and the Mod-*n*-CTA models (where $n = 1, 2$ or 3) as selector was simulated by MolInE docking program [28] (see also the subsection 1c in Computational Methods) that works on rigid molecular geometries. In the first step the Bz molecule is systematically moved towards the Mod-*n*-CTA system along different directions, until the two van der Waals surfaces come in contact. In the second step the interaction between the two partners is

optimized by a simplex procedure that searches for minimum energy configurations through small rotation-translation movements of the Bz molecule over the surfaces of Mod-*n*-CTA. During the docking process, the directions of approach of Bz are selected in such a way that the surfaces of the Mod-*n*-CTA models are adequately and homogeneously explored. In addition, for each of these directions, the orientation of the Bz molecule is repeatedly changed as it approaches the Mod-*n*-CTA surface. Finally, an energy- and structure-based selection is made and only the original low energy adducts are carried out to the next step where $\Delta\delta_H$ values are eventually calculated. In particular, the structural selection is performed by a specialized tool (the alignment of the candidates is based on the calculated principal moments of inertia for Mod-*n*-CTA) implemented in the stand-alone computer program CAT (Conformational Analysis Tools, see subsection 4 in Computational Methods for more details).

Calculation of diamagnetic anisotropy effects

We used the classic McConnell Equation (1) to estimate the $\Delta\delta_H$ values for H1′, H1–4 in the adducts formed by Bz and Mod-*n*-CTA models:

$$\Delta\delta_{Hcal} = \mu(1 - 3\cos^2\theta)/R^3 \quad (1)$$

In this equation, that treats the anisotropy effects according to the equivalent dipole model, R is the distance of a given H from the center of the Bz ring, θ is the angle formed by the vector R and the C_6 symmetry axis of Bz and μ is the magnetic dipole equivalent associated to the Bz molecule. The exact value of μ to be used in Equation (1) was found in the following way. First, three reference molecular structures were chosen to test the ability of our Mod-*n*-CTA models to reproduce the effect of magnetic anisotropy of the Bz nucleus: the reference structures are [6]- and [10]-paracyclophanes [31, 32] and the benzene–methane adducts [32] shown in Figure 2.

For these we calculated the $\Delta\delta_{Hcal}$ values of the hydrogens shielded (or deshielded) by the Bz rings using Equation (1) and varying values of μ. The chemical shifts δ_{Hcal} were in turn obtained by adding these values to the corresponding chemical shifts δ^r_H (Table 1) calculated (see subsection 3 in Computational Methods) for the same reference structures, devoid of diamagnetic anisotropy effects.

The latter (Figure 3) were obtained, from the isolated methane molecule (*RS-3*) and from [6]- and [10]-paracyclophanes (*RS-m*[6] and *RS-m*[10] with *m* equal to 1 or 2) by replacing their Bz rings with: (a) a cyclohexane fragment (evaluation of the δ^r_H for the aliphatic hydrogens); (b) a 1,3-cyclohexadiene (evaluation of the δ^r_H for the aromatic hydrogens).

Finally, the correct value for the parameter μ was chosen as the one giving the minimum mean

Table 1. Calculated chemical shift δ^r_H for the hydrogen atoms on the reference molecular structures devoid of diamagnetic anisotropy effects.

Hydrogen	*RS-m*-[6] (m = 1 or 2) δ^r_H(ppm)	*RS-m*-[10] (m = 1 or 2) δ^r_H(ppm)	*RS-3*
H—CH_3	–	–	0.27
Ha	1.46	1.45	–
Hb	1.46	1.46	–
Hc	1.46	1.55	–
Hd	1.46	1.51	–
He	1.55	1.45	–
Hf	1.55	–	–
Hn	5.82	5.82	–

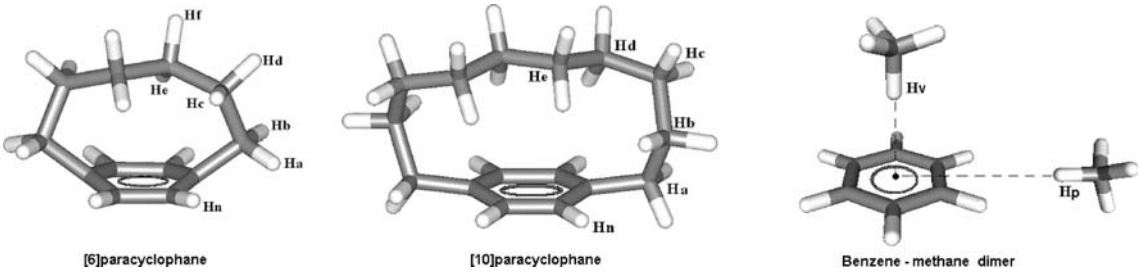

Figure 2. Reference molecular structures.

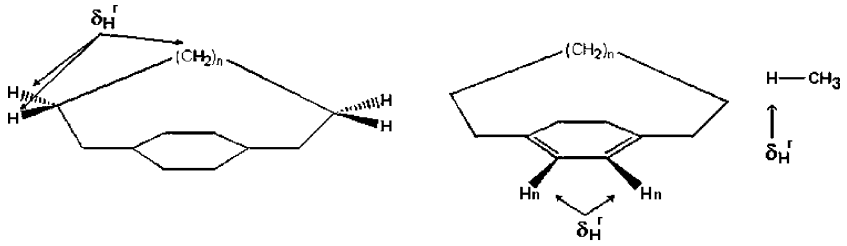

Figure 3. Reference molecular structures devoid of diamagnetic anisotropy effects.

square deviation ($\sigma[\delta_{Hexp}-\delta_{Hcal}]$, where δ_{Hexp} are the experimental values listed in Table 2. The values for the σ $[\delta_{Hexp}-\delta_{Hcal}]$ quantity, listed in Table 2, show that the calculated $\Delta\delta_{Hcal}$ values are quite accurate when a value of $\mu = 22$ ppm Å^3 is used in Equation (1) thus confirming the validity of our procedure. The $\Delta\delta_H$ for the H1′ and H1–4 hydrogens in the Mod-*n*-CTA//Bz models have been then calculated as Boltzmann weighted averages of the $\Delta\delta_H$ values computed for the individual Mod-*n*-CTA//Bz adducts.

Table 2. Estimated effects of magnetic anisotropy of the Benzene nucleus.

	δ_{Hexp} (ppm)	δ_{Hcal} (ppm)			
		$\mu = 32$	$\mu = 27$	$\mu = 22$	$\mu = 19$
[10]paracyclophane					
Ha	2.63	2.17	2.06	1.95	1.88
Hb	1.55	1.66	1.63	1.60	1.58
Hc	1.08	1.36	1.39	1.42	1.44
Hd	0.70	0.42	0.59	0.76	0.86
He	0.51	0.76	0.87	0.97	1.04
Hn	7.04	7.85	7.53	7.21	7.03
$\sigma[\delta_{Hexp}-\delta_{Hcal}]$		0.43	0.37	0.37	0.41
[6]paracyclophane					
Ha	1.97	2.05	1.95	1.86	1.80
Hb	2.79	2.12	2.02	1.91	1.85
Hc	1.58	1.17	1.21	1.26	1.29
Hd	0.51	0.95	1.03	1.08	1.16
He	0.62	−0.12	0.14	0.41	0.56
Hf	1.06	0.73	0.87	0.99	1.07
Hn	7.26	7.84	7.52	7.21	7.02
$\sigma[\delta_{Hexp}-\delta_{Hcal}]$		0.51	0.44	0.42	0.46
Benzene–methane dimer					
Hp	−2.88	−4.80	−3.45	−2.71	−2.20
Hv	0.71	0.71	0.60	0.52	0.48
$\sigma[\delta_{Hexp}-\delta_{Hcal}]$		1.36	0.41	0.19	0.51
$\sigma[\delta_{Hexp}-\delta_{Hcal}]_{med}$		0.77	0.41	0.33	0.46

Comparison between experimental δ_{Hexp} and calculated δ_{Hcal} chemical shift values of hydrogen atoms on the reference molecular structures.

Results and discussion

It is well established that the position of NMR signals (δ_{Obs}) of two species undergoing a fast reversible association process are the weighted average values representing both free (δ_{Free}) and complexed species (δ_{Comp}), according to Equation (2):

$$\delta_{Obs} = \delta_{Free} \times X_{Free} + \delta_{Comp} \times X_{Comp} \qquad (2)$$

where X_{Free} and X_{Comp} are the molar fractions of free and complexed species, respectively. Accordingly, the chemical shift value δ_{Obs} of each proton of CTA in the systems composed by CTAX and Bz molecules will be a function of their relative concentrations, a parameter that in turn may have an influence on the degree of complexation. A quantity that is related to the observed values δ_{Obs} but is not dependent on the molar fractions of free and complexed CTA, can be derived using the ratios $R\delta_H^{h/k} = \Delta\delta_{Hh} / \Delta\delta_{Hk}$, where h and k refer to anisochronous protons within the CTA molecule. Using $X_{Free} = 1-X_{Comp}$ in Equation (2) and rearranging, one obtains for a generic proton j of the CTA molecule:

$$\delta_{Hobsj} - \delta_{Hfreej} = \Delta\delta_{Hobsj} = X_{Comp} \times (\delta_{Compj} - \delta_{Hfreej}) \qquad (3)$$

The independence of the ratio $R\delta_H^{h/k}$ on X_{Free} e X_{Comp} is expressed by Equation (4):

$$R\delta_{\mathrm{H}}^{h/k} = \Delta\delta_{\mathrm{Hobs}h}/\Delta\delta_{\mathrm{Hobs}k} = (\delta_{\mathrm{Comp}h} - \delta_{\mathrm{HFree}h})/(\delta_{\mathrm{Comp}k} - \delta_{\mathrm{HFree}k}) \quad (4)$$

We have calculated, as independent properties for the complexes formed in 0.1 M CTAX micelles and variable concentrations of Bz, the pertinent ratios $R\delta_{\mathrm{H}}^{h/k}$ (Table 3).

As expected, these values are independent on the Bz concentration (Figure 4) and are not affected by the nature of the counterion in CTA (Table 4).

Their averaged value was thus taken as a reference point to be used in the study of the location of Bz on the micelle surface.

Studies using the model Mod-1-CTA

The rigid docking procedure gave 51 different minimum-energy Mod-*1*-CTA//Bz adducts, in an energetic window of 6 kcal mol^{-1}. These were used to first calculate $\Delta\delta_{\mathrm{Hcalc}}$ values for the hydrogens H1′, H1, H2, H3 + H4, and then the ratios $R\delta_{\mathrm{H}}^{h/k}$ (Table 3). The computations were performed using seven different values of Z_{CO} and excluding iteratively from the initial pool of 51 geometries those found to not conform to the geometrical constraints imposed to the Bz molecule. The values of $\Delta\delta_{\mathrm{Hcalc}}$ were then calculated only for the so selected Mod-*1*-CTA//Bz adducts. Results clearly indicate that the difference between calculated and observed data changes with Z_{CO}, reaching a minimum value at Z_{CO} = 3.8–4.0 Å (Figure 5).

Table 3. Experimental and calculated $R\delta_{\mathrm{H}}^{h/k}$ ratios.

Mod-*1*-CTA//Bz		Cutoff Z_{CO} (Å)						
		5.2	4.5	4.3	4.0	3.8	3.0	2.5
h/k	$R\delta_{\mathrm{Hexp}}^{h/k}$				$R\delta_{\mathrm{Hcal}}^{h/k}$			
H2/H1	1.08	1.58	1.13	0.94	0.75	0.75	0.52	0.45
H1/H3 + 4	1.27	0.38	0.58	0.78	1.22	1.22	1.07	6.34
H2/H3 + 4	1.37	0.60	0.66	0.73	0.92	0.92	3.36	2.83
H1/H1′	1.79	4.97	3.65	2.76	2.42	2.42	1.85	1.95
H2/H1′	1.93	7.83	4.13	2.59	1.82	1.82	0.97	0.87
H1′/H3 + 4	0.71	0.08	0.16	0.28	0.50	0.50	3.46	3.25
$\sigma[R\delta_{\mathrm{Hexp}}^{h/k} - R\delta_{\mathrm{Hcal}}^{h/k}]$	–	2.80	1.26	0.61	0.35	0.35	1.46	2.45
Mod-*2*-CTA//Bz								
h/k	$R\delta_{\mathrm{Hexp}}^{h/k}$	$R\delta_{\mathrm{Hcal}}^{h/k}$						
H2/H1	1.08	1.30						
H1/H3 + 4	1.27	10.37						
H2/H3 + 4	1.37	13.43						
H1/H1′	1.79	1.98						
H2/H1′	1.93	2.57						
H1′/H3 + 4	0.71	5.23						
$\sigma[R\delta_{\mathrm{Hexp}}^{h/k} - R\delta_{\mathrm{Hcal}}^{h/k}]$	–	6.45						
Mod-*3*-CTA//Bz								
h/k	$R\delta_{\mathrm{Hexp}}^{h/k}$	$R\delta_{\mathrm{Hcal}}^{h/k}$						
H2/H1	1.08	1.66						
H1/H3 + 4	1.27	0.31						
H2/H3 + 4	1.37	0.51						
H1/H1′	1.79	3.75						
H2/H1′	1.93	6.22						
H1′/H3 + 4	0.71	0.08						
$\sigma[R\delta_{\mathrm{Hexp}}^{h/k} - R\delta_{\mathrm{Hcal}}^{h/k}]$	–	2.02						

Experimental data are referred to CTAS micellar aggregates.

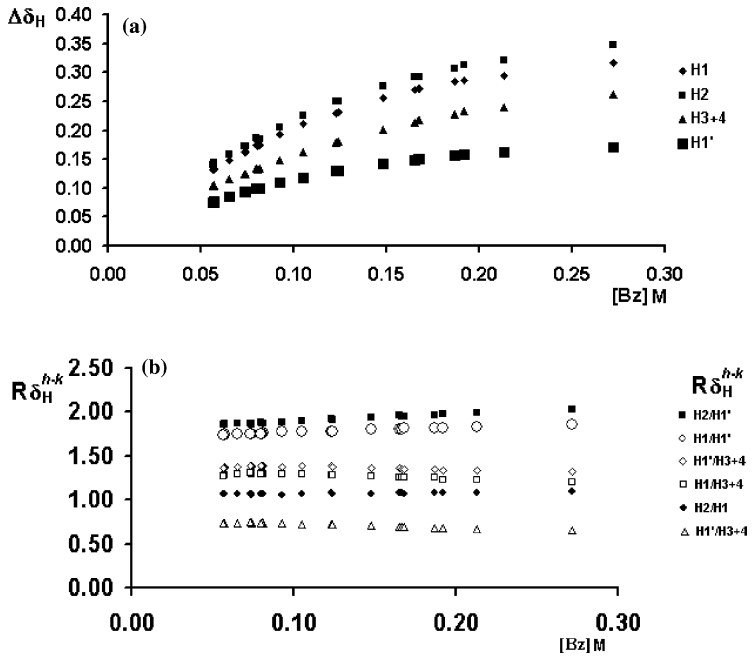

Figure 4. Experimental variation of chemical shift induced by complexation between Bz and CTAS micelles. (a) dependence of the induced shift on Bz concentration; (b) independence of the $R\delta_H^{h/k}$ ratios on Bz concentration.

The sliding of the Bz molecule towards the interior of the micellar system up to 4.0 Å away from the cationic head can be taken as the maximum allowed distance the Bz molecule can travel along the CTA alkyl chains maintaining favorable interactions with the hydrocarbon fragments. The Bz molecule is found preferentially over C2 and C3 carbons, about 3.9 Å away from the charged nitrogen atom (global minimum, Figure 6a), and with the aromatic ring plane arranged orthogonally to the C—H bonds to favor a classical VdW C–H$\cdots\pi$ interaction.

Table 4. Independence of the $R\delta_H^{h/k}$ ratios on the CTA counterion nature.

h./k	$R\delta_{Hexp}^{h/k}$				
	CTAB	CTAN	CTAS	CTAC	CTAMs
H2/H1	1.1	1.0	1.1	1.1	1.1
H1/H3 + 4	–	–	1.3	1.2	1.3
H2/H3 + 4	–	–	1.4	1.3	1.4
H1/H1′	1.9	1.9	1.8	1.8	1.8
H2/H1′	2.1	2.2	1.9	1.9	2.0
H1′/H3 + 4	–	–	0.7	0.7	0.7

Studies using the model Mod-2-CTA

Molecular docking gave in this case 52 different minimum-energy Mod-*2*-CTA//Bz adducts, in an energetic window of 6 kcal mol^{-1}. All of them were used for the calculations of $\Delta\delta_{Hcalc}$ values and of the related $R\delta_H^{h/k}$ ratios. The results show that this model of the micelle is not suited for the accurate reproduction of experimental data. Analysis of the deviations between calculated and observed $R\delta_H^{h/k}$ values indicates that the model systematically underestimate the $\Delta\delta_{Hcalc}$ values for

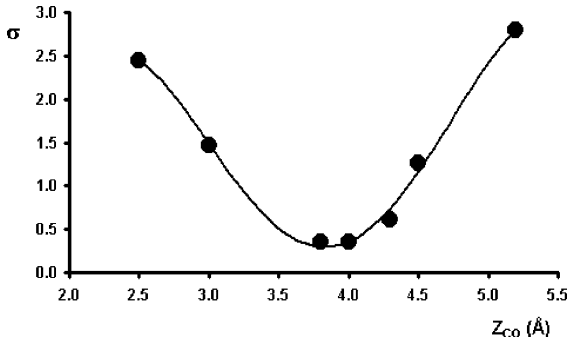

Figure 5. Estimated sliding of the Bz molecule towards the interior of the micelle using Mod-*1*-CTA model.

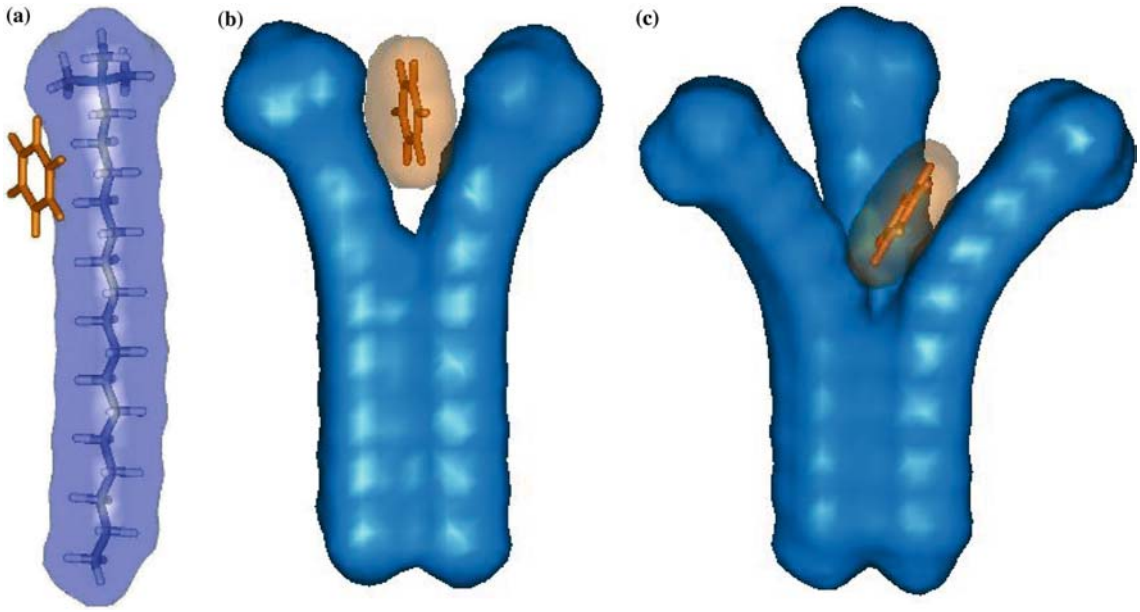

Figure 6. Global minima of the complexes Mod-*n*-CTA/Bz. (a) Mod-*1*-CTA/Bz; (b) Mod-*2*-CTA/Bz; (c) Mod-*3*-CTA/Bz.

the hydrogens on carbons C3 and C4, suggesting that this model prevents the deep insertion of the Bz molecule between the almost undissociated alkyl chains (Figure 6b). In the global minimum, the Bz molecule reaches its maximum distance from the nitrogen atom at about 2.6 Å. On the other hand, the ratios obtained from the $\Delta\delta_{\mathrm{Hcalc}}$ values for the H1′, H1 and H2 hydrogens are in good agreement with the experimental data. In the low energy Mod-*2*-CTA//Bz adduct, the aromatic ring is almost symmetrically oriented towards the two alkyl chains in order to maximize the contact surface area of the two species.

Studies using the model Mod-3-CTA

The presence of a third CTA unit in the Mod-*3*-CTA model induces considerable repulsion between the charged headgroups and this in turn leads to a pronounced divergence of the alkyl chains. As a consequence, the docking procedure gave, in an energetic window of 6 kcal mol^{-1}, 47 minimum energy geometries for the Mod-*3*-CTA// Bz adducts whose calculated $R\delta_{\mathrm{H}}^{h/k}$ are closer to experimental ones than those of Mod-*2*-CTA. However, the results of Mod-*3*-CTA are still worse than those obtained with Mod-*1*-CTA.

The wide pocket generated between the cationic heads of CTA allows a deeper insertion of the aromatic ring within the modeled micelle, as evidenced by the small differences between calculated and observed values for the $R\delta_{\mathrm{H}}^{h/k}$ ratios of H1, H2, and H3 + H4 hydrogens (Table 3). Nonetheless, the extent of insertion appears to be overestimated (in the global minimum the distance from each of the nitrogen atoms is about 6.5 Å, Figure 6c) and systematically gives unbalanced $R\delta_{\mathrm{H}}^{h/k}$ ratios in favor of the $\Delta\delta_{\mathrm{H}}$ values for the H3 and H4 hydrogens. This is in turn reflected in a low quality of the $\Delta\delta_{\mathrm{Hcalc}}$ values for the H1′ hydrogens that appear largely underestimated (see the ratios $R\delta_{\mathrm{H}}^{2-1'}$ and $R\delta_{\mathrm{H}}^{1-1'}$, Table 3). The reason of the non-optimal behavior of Mod-*3*-CTA is that a large proportion of adduct geometries locate the Bz molecule over the H3 and H4 hydrogens, far away from H1′, and this is reflected in a small contribution to the diamagnetic anisotropy experienced by H1′ hydrogens. In addition, a poor sampling density at the surface of the headgroup methyls during the rigid docking phase could explain the underestimation of the $\Delta\delta_{\mathrm{H}}$ values for the H1′ hydrogens.

In the low energy structure of the Mod-*3*-CTA//Bz adducts, the Bz molecules is located at the divergence point of the alkyl chains, where the largest contact between the molecular surfaces is realized. The aromatic ring is oriented in a non-symmetrical manner inside the tripod of

Mod-*3*-CTA, resting on the surface of one alkyl tail with the aryl ring perpendicular to the C—H bonds most likely to favor a C—H$\cdots\pi$ interactions (Figure 6b, c). This relative disposition resembles that observed with Mod-*1*-CTA model.

Comparison of the results provided by the three models indicates that the simple Mod-*1*-CTA gives a better reproduction of experimental data. This finding suggests that in the real system the charged heads of CTA repel each other and force the alkyl chains to straddle up to the point that a small, flat molecule like Bz can intercalate easily up to the first apolar portion of the alkyl chains of CTA. Consequently, we believe that in spite of its oversimplifications Mod-*1*-CTA model can be effectively used, in combination with classical docking procedures, to study other molecular recognition phenomena operated by surfactants with charged headgroups. For the remaining two Mod-*2*-CTA and Mod-*3*-CTA models, the results indicate as a major limit their inability to correctly reproduce the distance between the charged heads and the induced separation of the alkyl chains. This in turn leads to under- or over-estimate the sliding of Bz towards the interior of the micelle (about 25% of the value calculated with Mod-*1*-CTA). A second limitation of the models with two and three CTA units is related to the increased computational demand of the docking procedure due to the large number of heavy atoms of the systems.

The principal indication obtained from our studies is that in the real system the Bz molecules prefer to stay adjacent to the polar heads of CTA and close to the point at which the alkyl chains begin to diverge. This supramolecular arrangement, in which the Bz is partially buried inside the micelle, maximizes VdW interactions that are proportional to the contact surface area of the species.

Accordingly, we believe that Mod-*3*-CTA can be improved by modulating the extent to which the alkyl chains tend to diverge under the effect of head–head repulsion. This result could be achieved by using a proper value for the dielectric constant ϵ, (e.g. intermediate between that of pure water and that of vacuum) during the docking simulation.

Conclusions

We used a computational approach to reproduce experimental ^{1}H-NMR chemical shift data for systems composed by solubilized Bz in aqueous solutions of cetyltrimethylammonium surfactants. Three simplified models of the micelles were used in the computation, and the ^{1}H-NMR data were extracted by combining a docking routine with a chemical shift prediction module.

With the simple Mod-*1*-CTA model our approach correctly reproduced the experimentally observed chemical shift values. This work suggests a general protocol for the study of micelle-based supramolecular systems with relevance to chemical catalysis or molecular recognition.

References

1. Chasman D.I., Protein Struct., 417 (2003).
2. Lipkowitz, KB., J. Chromatogr. A., 906 (2001) 417.
3. Shoichet, B.K., Mc Govern, S.L., Wai, B. and Irwin, J., Curr. Opin. Chem. Biol., 6 (2002) 439.
4. Cui, M., Huang, X., Luo, X., Briggs, J.M., Ji, R., Chem, K., Shen, J. and Jiang, H., J. Med. Chem., 45 (2002) 5249.
5. Burkhard, P., Hommel, V., Sanner, M. and Walkinshaw, M.D., J. Mol. Biol., 287(5) (1999) 853.
6. Gschwend, D.A., Good, A.C. and Kuntz, I.D., J. Mol. Recogn., 9(2) (1996) 175.
7. Lipkowitz, K. B., Acc. Chem. Res., 33 (2000) 555.
8. Mittol, K.L. (Ed.) Micellization, Solubilization and Microemulsions, Vol. 1, Plenum Press, New York, 1997.
9. Fendler, J. and Fendler, E., Catalysis in Micellar and Macromolecular Systems, Academic Press, New York, 1975.
10. Wasan, D.T., Ginn, M.E. and Shah, D.O. (Eds.) Surfactants in Chemical/Process Engineering, Dekker, New York, 1988.
11. Herman, D.C., Artiola, J.F. and Miller, R.M., Environ. Sci. Technol., 29 (1995) 2280.
12. Cerichelli, G., Cerritelli, S., Chiarini, M., De Maria, P. and Fontana, A., Chem. Eur. J., 8 (2002) 5204.
13. Kabir-ud-Din ., Kumar, S. and Goyal, P.S., Langmuir, 12 (1996) 1496.
14. Duns, G.J., Reeves, L.W., Yang, D.W. and Williams, D.S., J. Colloid Interf. Sci., 173 (1995) 261.
15. Mukerjee, P. and Cardinal, J.R., J. Phys. Chem., 82 (1978) 1620.
16. Pauling, L., J. Chem. Phys., 4 (1936) 673.
17. Haigh, C.W. and Mallion, R.B., Progr. Nucl. Magn. Reson. Spectrosc., 13 (1980) 303.
18. Stamm, H. and Jäckel, H., J. Am. Chem. Soc., 111 (1989) 6544.
19. Fleisher, U., Kutzelnigg, W., Lazzaretti, P. and Mühlenkamp, V., J. Am. Chem. Soc., 116 (1994) 5289.
20. Pople, J.A., J. Chem. Phys., 24 (1956) 1111.
21. Wangh, J.S. and Fessenden, R.W., J. Am. Chem. Soc., 79 (1957) 846.
22. Johnson, C.E. and Bovey, F.A., J. Chem. Phys., 29 (1958) 101.
23. Abraham, R., J. Mol. Phys., 4 (1961) 145.
24. Abraham, R.J. and Medforth, C.J., Magn. Reson. Chem., 25 (1987) 432.

25. Cochran, J.E., Parrott, T.J., Withlock, B.S. and Withlock, H.W., J. Am. Chem. Soc., 114 (1992) 2269.
26. Schneider, M.J., Ree. Trav. Chim. Pays-Bas, 112 (1993) 412.
27. Cerichelli, G. and Mancini, G., Langmuir, 16 (2000) 182.
28. Alcaro, S., Gasparrini, F., Iucani, O., Mecucci, S., Misiti, D., Pierini, M. and Villani, C., J. Comput. Chem., 21 (2000) 515.
29. Bruce, C.D., Berkowitz, M.L., Perera, L. and Forbes, M.D.E., J. Phys. Chem. B, 106 (2002) 3788.
30. Tieleman, D. P., van der Spoel, D. and Berendsen, H. J. C., J. Phys. Chem. B,, 104 (2000) 6380.
31. Abraham, R.J., Canton, M., Reid, M. and Griffiths, L., J. Chem. Soc., Perkin Trans., 2 (2000) 803.
32. Alkorta, I. and Elguero, J., New J. Chem., (1998) 381.